



1 **Reply to Comment on Franz et al. (2023): A reinterpretation of the 1.5 billion year old Volyn**
2 **'biota' of Ukraine, and discussion of the evolution of the eukaryotes, by Head et al. (2023)**

3
4 **Gerhard Franz¹, Vladimir Khomenko^{1,2}, Peter Lyckberg³, Vsevolod Chornousenko⁴, Ulrich**
5 **Struck⁵**

6 ¹Institut für Angewandte Geowissenschaften, Technische Universität Berlin, D-10587 Berlin,
7 Germany

8 ²M.P. Semenenko Institute of Geochemistry, Mineralogy and Ore Formation, The National
9 Academy of Sciences of Ukraine, 34, Palladina av., Kyiv, 03142, Ukraine

10 ³Luxembourg National Museum of Natural History, 25 Rue Münster, 2160 Luxembourg,
11 Luxembourg

12 ⁴Volyn Quartz Samotsvety Company, Khoroshiv (Volodarsk-Volynski), Ukraine*

13 ⁵Museum für Naturkunde, Leibniz-Institut für Evolutions- und Biodiversitätsforschung,
14 Invalidenstraße 43, Berlin, D-10115, Germany

15 *now at: Kondratyuka str. 9, al. 25, Zhytomyr, 10009 Ukraine

16

17 Correspondence: Gerhard Franz (gerhard.franz@tu-berlin.de; gefra548@gmail.com)

18

19 **Abstract.** Head et al. (2023) emphasize the importance of the Volyn biota for the evolution,
20 especially in the so-called 'boring billion', in a detailed outline about the biological and
21 geological context. However, they question that the Volyn biota represent Precambrian fossils
22 and instead argue that they are young contaminants of 'museum dust'. In addition, they
23 postulate that they are of a-biotic origin. We present here a detailed discussion of their points
24 of concern based on presented data, including some additional information. Their points of
25 concern were:

- 26 - One object, shown by Franz et al. (2023) is similar to a pollen grain, another object is
27 similar to trichomes; we show indications for fossilization and summarize our
28 arguments against 'museum dust'.
29 - They question the fossil character of the biota and argue for a biomineralization; we
30 show that the biomineralization in trichomes is distinct from the mineralization of the
31 biota.
32 - They missed information about the internal structure; we repeat the presented
33 information about the internal structure in more detail, which is also indicative of fossil
34 material and inconsistent with trichomes.
35 - They argue that we did not compare via infrared spectroscopy the biota with recent
36 fungi; since the biota experienced temperatures near 300°C, we think that a
37 comparison with thermally degraded chitosan is more appropriate.
38 - They question the use of strongly negative $\delta^{13}\text{C}$ as an argument for biotic origin, but
39 we show that in combination with positive $\delta^{15}\text{N}$ values and the geological situation, a
40 biotic origin is more likely than abiotic synthesis.

41 In addition, Popov (2023) questioned the age of the Volyn biota, which we postulated as
42 between approximately 1.5 and 1.7 Ga. He argues that the fossils could be Phanerozoic. We
43 will also outline our arguments for the minimum age of 1.5 Ga.

44

45 **1 Introduction**



46 We thank Head et al. (2023) for stimulating the discussion about the Volyn biota. They
47 question that these are fossils, instead argue that at least some of them are young
48 contaminants by plant hairs and pollen. This could have occurred during storage as what they
49 called ‘museum dust’ or during sampling. Furthermore, they question the biogenicity and
50 argue for an abiotic origin. We appreciate their comment, because this question of
51 contamination was not raised before, neither in our papers from 2017, 2022, and 2023, nor in
52 any of the previous publications about kerite who either described kerite as an abiogenic
53 material (Ginzburg et al., 1987; Luk’yanova et al., 1992; Yushkin 1996, 1998) or as fossilized
54 cyanobacteria (Gorlenko et al., 2000; Zhmur, 2003).

55

56 **2 Occurrence of kerite and sampling**

57 The following information is based on logbooks from the mine (VC, mine geologist in the area
58 since 1990) who also collected the material for our study together with PL. The samples of
59 kerite occur in situ underground in several, but not all shafts of the Volyn pegmatite district.
60 Within the large, miarolitic cavities (‘chambers’ in the original literature) kerite is also found
61 in the mineral matrix (feldspar, mica, clay minerals) on the floor of the pegmatite and is also
62 hanging from the walls or the ceiling. However, kerite in visible amounts is not preserved in
63 most chambers. It was either destroyed during cleaning and gemstone extraction, or it was
64 already collected. In those chambers which were explored by drilling, it was completely
65 destroyed by drilling fluids mixed with clay that covered the whole ground of the chambers.
66 Well-preserved large amounts of kerite were found only in new pockets opened by miners
67 underground without drilling. In January 2013 kerite was found (PL) in a 5 mm wide zone
68 around topaz crystals on the wall of a 15 m tall chamber in shaft 3. Kerite was observed
69 growing at the base of dark lilac black fluorite crystals, in larger fiber masses around large
70 topaz crystals, as larger fiber masses in clay along the lower walls and as large masses on well
71 crystallized feldspars, mica, quartz and topaz high on the walls in two chambers.

72 Early descriptions in the drilling logbooks mention in some cases that chambers were full
73 of kerite, up to 25 kg of kerite(!) in the rather small pegmatite body from shaft 3, which has
74 accesses to several pegmatite bodies (consistent with reports in the literature, e. g. Ginzburg
75 et al., 1987). Material from this shaft was distributed to museums in the former Soviet Union.
76 The chambers are now in a depth of up to 96 m, some were mined in open pits, but the
77 crystallization depth of the pegmatites was at a depth corresponding to 2-3 kbar. Thus,
78 significant uplift had occurred since intrusion at 1.76 Ga, but there is no indication from the
79 geological literature of the area that the chambers were directly on or beneath the surface
80 and buried again later. Therefore, contamination within the chambers by plant roots going
81 down to 96 m is less likely. In any case, we have no doubt that kerite is part of the deep
82 biosphere. Most trichomes (plant hairs) are known from plants on the surface, not from deep
83 biosphere.

84 Samples kerite 1 to kerite 7 were sampled underground by PL and VC, put into firmly
85 closed plastic sample bags (double ones with label in outer one), transported first to
86 Luxemburg and then sent to Berlin. There was no need to separate kerite from the rocks and
87 from the soil, the material could be picked up. Sample bags were opened only in the electron
88 microscopy laboratory of TU Berlin, which is a special building for electron microscopy with
89 the appropriate arrangements to prevent contamination by dust. All rooms are equipped with
90 airlocks for climatization and in addition water-cooled ceilings minimizes airstream and dust
91 movement in the rooms. Samples were prepared in an exhaust hood. Of course, we cannot
92 completely rule out that some objects are contaminants, but the overwhelming majority of
93 objects on the aluminum sample holders for scanning electron microscopy (SEM) are original



94 as recovered from underground. The only kerite sample, which could have been contaminated
95 in a museum is our sample 'kerite 0'.

96 The beryl crystal sample V2008 was collected from the mine tailings in 2008 by GF, stored
97 at TU Berlin in a common wooden rock cabinet. For this sample, contamination on the mine
98 tailings or later is possible.

99 The breccia with the beryl pseudomorph was also collected from the mine tailings in 2008
100 by GF, stored at TU Berlin in a common wooden rock cabinet, and consolidated with epoxy for
101 preparation of thin sections and polished blocks for the Ar-Ar-determination of muscovite.

102

103 **3 Composition and structure of kerite**

104 **3.1 Organic matter in the beryl pseudomorph**

105 We start the discussion with the OM in the pseudomorph. For this, a later contamination can
106 safely be excluded, as it was discovered in thin sections. It is closely surrounded and
107 intergrown with macroscopically black, in thin section brown, C-H-bearing opal (Franz et al.
108 2017; see their fig. 6). The chemical composition of the OM is characterized by a high amount
109 of Zr, Y, Sc, and REE. These high fieldstrength elements (HFSE) are positively correlated with
110 O, and increasing O contents are correlated with decreasing C contents. The N content is
111 between 2 and 4 at%, much lower than the original kerite (see their fig. 7), which has near 8-
112 9 at% (Ginzburg et al., 1987; Yushkin, 1996). Mobilization of HFSE is possible with a F-rich fluid
113 (Loges et al. 2023), and a high F-content in the system is likely because the pegmatites
114 themselves belong to the Nb-Y-F-type and contain a high amount of topaz. In addition, the
115 muscovite in the breccia is F-rich, and fluorite is a common mineral associated with kerite (see
116 below). For further details such as transmission electron microscopy of the border zone of OM
117 to opal and about opal itself, the reader is referred to our original publication.

118 We postulated that the low N-content was caused by decay of kerite, producing NH_4 ,
119 which was responsible for K- NH_4 exchange reactions in K-feldspar and in muscovite, forming
120 buddingtonite and tobelite. There is no doubt that before the formation of the breccia and
121 the pseudomorph, OM was present in the system. Buddingtonite is not a rare mineral in the
122 Volyn pegmatite field (Proshko, 1987) and the high activity ratio for NH_4^+/K^+ required to
123 transform K-feldspar into buddingtonite (Mäder et al., 1996) indicates a large amount of
124 decayed OM. This is not consistent with Head et al.'s concern that the OM in the pegmatite
125 field is late-stage contamination. Also, the chemical composition of the OM is completely
126 incompatible with anything like museum dust or plant hairs.

127

128 **3.2 Fossil or non-fossilized OM**

129 Head et al. (2023) question the fossil character of kerite. Here we want to summarize the
130 presented information about the metamorphic, mature character of kerite.

131 After the occurrence of OM in the pegmatitic environment, the temperatures had
132 reached again approximately 300 °C (Franz et al. 2017). This estimate is based on the phase
133 equilibria with bertrandite and muscovite in the pseudomorph. Furthermore, within beryl we
134 observed fluid inclusions with C-H, which occur on cracks sealed by secondary beryl (Voszniak
135 et al., 2012). This implies that temperatures were above the lower thermal stability of beryl,
136 which is at low pressure near 300 °C (Barton and Young, 2002). These temperatures are
137 consistent with our observation on decomposition of chitin to chitosan described in detail in
138 Franz et al. (2023a), see below the discussion about FTIR data.

139 All kerite samples were investigated by open-system pyrolysis. They do not differ
140 significantly, and all spectra show characteristics of mature to very mature OM (figure 13 in
141 Franz et al. 2022, and in supplement). This excludes young contamination by plant hairs.



142 Similarly, the light microscopic investigations in cross sections with white and UV light show
143 clear indications by different reflectivity and fluorescence, not consistent with young OM. We
144 described brittle behavior of kerite, also not compatible with young unmetamorphosed OM.
145 Brittle behavior was also noted by Yushkin (1996). Luk'ynaova et al. (1982) described X-ray
146 diffraction investigations with a diffuse peak at 8° Theta indicating OM with some graphite-
147 like sheets.

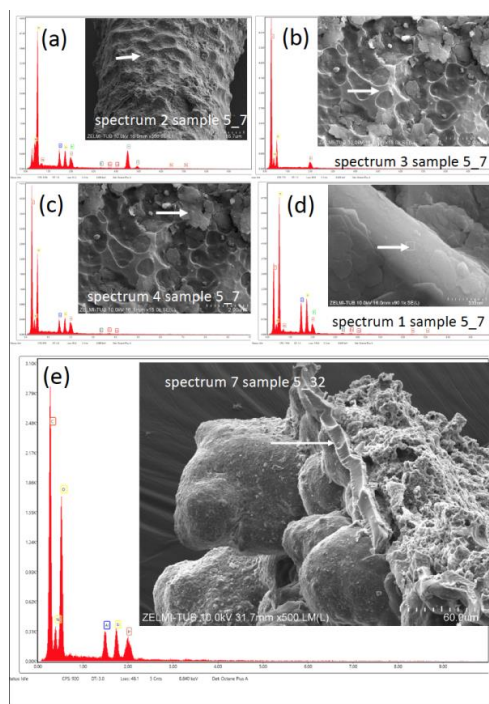
148 Head et al. (2023) refer to mineralized trichomes (Mustafa et al. 2017, 2018; Ensikat et al.
149 2017) and take this as an argument against fossilization. These plant hairs are biomineralized
150 with Ca-carbonate, Ca-phosphate and silica, especially at the tip of the trichomes. This
151 biomineralization is quite different from what we interpreted as fossilized and mineralized
152 rims of the Volyn kerite. We wrote that the most conspicuous feature is the common
153 occurrence of Si-Al-O, interpreted as Al-silicates. In the quoted investigations Al was never
154 observed. Furthermore, Ca-phosphate was observed in kerite only at some places at nano-
155 sized crystals (see e.g. figure 11 in Franz et al. 2022), at variance with a continuous
156 biomineralization on the tips. Kerite is completely surrounded by a mineralized rim, whereas
157 trichomes are only mineralized at their tips. All different kerite morphologies are mineralized
158 in the same way.

159 Concerning the analytical procedure applied by us, there is a misunderstanding in Head
160 et al.'s (2023) comment. On line 146 to 149 they wrote: "Had Franz et al. (2023) used EDX in
161 addition to applying EDAX EDS to selected cross sections, they would have been easily able to
162 determine the elemental distribution for all specimens they imaged using SEM which could
163 have assisted in discriminating extant contaminations from fossil material." For our element
164 mapping we used wave length dispersive (WDS) analysis with the electron microprobe (EMP),
165 which is much more sensitive than energy dispersive systems (EDS) such as EDAX. We have
166 shown several element distribution maps of different morphologies in Franz et al. (2022), and
167 since all show generally identical features with an Al-Si-Ca rim structure and an internal
168 structure with characteristic N-O-S distribution, we can safely exclude biomineralization, but
169 instead mineralization due to a fossilization process.

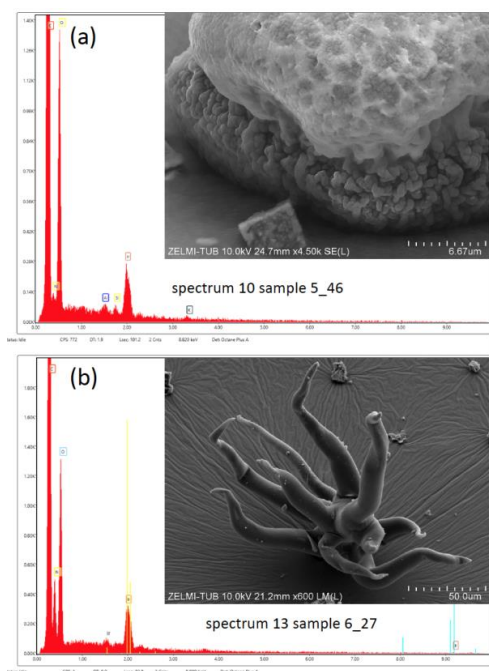
170

171 **3.3 EDS (with SEM)**

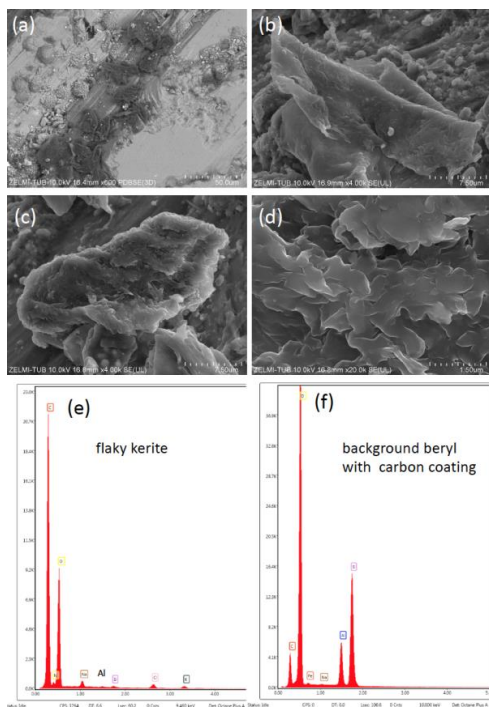
172 All spectra of kerite objects show a high amount of oxygen. This excludes fresh organisms but
173 indicates again (highly) mature OM. Minerals on the surface of filamentous kerite (Fig. 1a-d),
174 of bulbous kerite (Fig. 1e), and of the spherical object, interpreted by Head et al. (2023) as a
175 pollen, are mostly Al-silicates, some with K, Na, and Ca. The flaky shape of the minerals
176 indicates clay minerals, one needle-shaped crystal is a Ti-oxide, possibly rutile.



177
178 **Figure 1.** EDS spectra obtained with the SEM of filamentous (a, b, c, d) and bulbous (e) kerite
179 objects. (a) Needle-shaped small object with high Ti-O contents (arrow; interpreted as rutile)
180 next to Al-silicates with minor amounts of Na, K, and Ca. (b) Spectrum of clear surface (arrow)
181 of kerite, showing only the kerite composition of C-N-O. (c) Spectrum of platy mineral grains
182 (arrow) with Al-Si and small contents of K and Fe, interpreted as a clay mineral. (e) Base
183 (arrow) of bulbous kerite, with high amounts of Al-Si. Samples are iridium-coated.



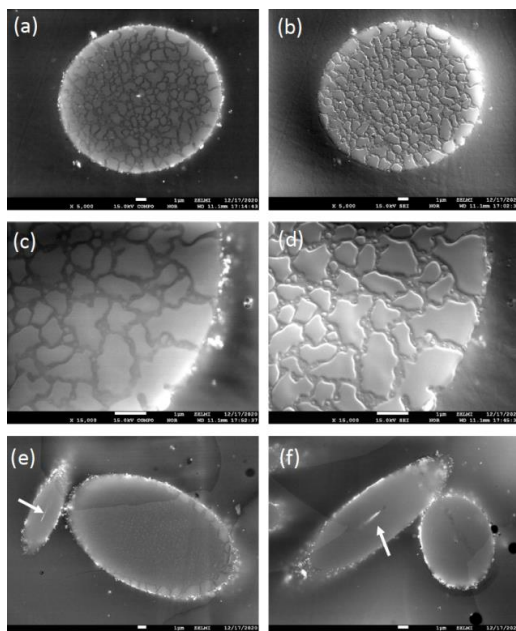
184
185 **Figure 2.** EDS spectra of a spherical object (a) and a filamentous object (b). The spherical object
186 shows Al-Si-K peaks, which can be interpreted as illite, whereas the filamentous object shows
187 only the typical composition of kerite with C-N-O; both samples are iridium-coated.
188



189



190 **Figure 3.** EDS data of flaky kerite, observed on sample V2008, a beryl crystal. (a, b, c, d) show
191 the structure of kerite, in (a) with combined BSE detector for element contrast. The dark
192 contrast compared to background beryl and other minerals indicates low average atomic
193 number. (e) is the corresponding EDS spectrum with clear indication for Si, Al, Na, K, and Cl,
194 next to C-N-O of kerite. (f) is EDS spectrum of beryl; note the low C-peak caused by carbon
195 coating, compared to the large C-peak of kerite.
196



197 **Figure 4.** BSE (a, c, d, e) and SE (b, d) of cross sections of filamentous kerite, embedded in
198 epoxy. Note the discontinuous rim of high contrast indicating mineralized parts, and within
199 the channel (e, f) also with high contrast (arrows). The mosaic pattern with different contrast
200 in BSE (a, c) is seen in SE images (b, d) as slightly lower areas of approximately 200 nm width.
201
202

203 The EDS spectrum of the object, interpreted as pollen by Head et al. (2023), also shows
204 the presence of Al and Si, together with the typical C-N-O peaks (Fig. 2). The EDS spectrum of
205 the object, interpreted by Head et al. (2023) as trichome 'museum dust' (Fig. 3) shows no Al-
206 Si, but the C-N-O ratios are very similar to those of the mineralized filaments, and therefore
207 we have no doubts that this is also fossilized OM.
208

209 3.4 EMPA data

210 In BSE images of cross sections of filamentous kerite we see a discontinuous mineralized rim
211 (Fig. 4). In combination with the element mappings (see images in figures 8 to 11 in Franz et
212 al. 2022, and figures S6, S7 in the supplement to Franz et al. 2022), we can safely conclude
213 that the mineralized rim consists dominantly of Al-silicates. Some other minerals such as Ca-
214 phosphate or silica occur only in isolated spots and do not cover the whole rim. Over a distance
215 of approximately 1 μm the filament shows a higher contrast rim in BSE images, indicating a
216 higher average atomic number, consistent with our interpretation that this is caused by a
217 mineralized, impregnated rim of dominantly Al-silicates. In the internal structure of the
218 filament, a mosaic pattern can be observed with approximately 200 nm wide channels, also



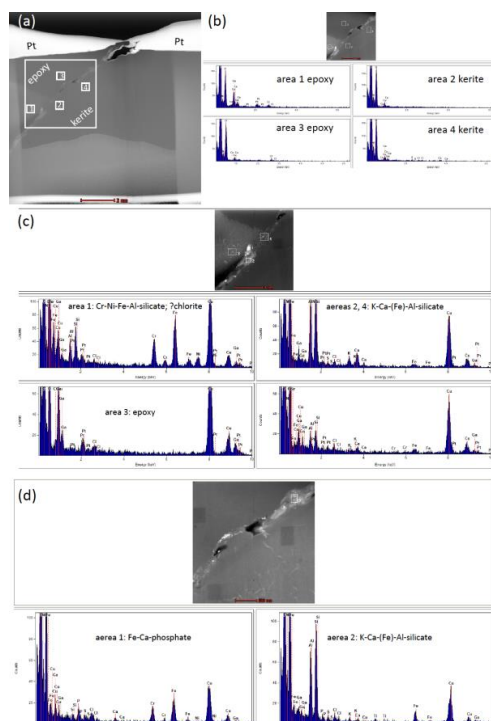
219 indicated by different element contrast (Fig. 4a, b). In SE images (Fig. 4c, d) a slightly lower
220 position of the channels is seen, caused by different behavior during polishing. This internal
221 structure is compatible with fossilized material, not with fresh cells of trichomes.

222

223 3.5 TEM data

224 In addition to the transmission electron microscope (TEM) investigations we presented in
225 Franz et al. (2017), we cut a new focused ion beam (FIB) foil from a filamentous object (Fig.
226 5). The foil covers the embedding material epoxy (characterized by typical Cl-content), the
227 approximately 500 nm wide rim and kerite (with dominantly C-O and N). The rim consists of a
228 mixture of different minerals, which can be distinguished by different contrast in the HAADF
229 images. EDAX spectra indicate dominantly Al-silicates with minor amounts of K, Ca, and Fe,
230 and a Fe-Ca-phosphate. This is different from the type of biomineralization in trichomes,
231 shown by Mustafa et al. (2017, 2018) and Ensikat et al. (2017).

232



233

234 **Figure 5.** Analytical EDAX-TEM results on a FIB from the rim of a filamentous kerite object.
235 Note for all spectra that Ga-peaks are due to the Ga ion cutting, Cu peaks originate from the
236 copper grid, and Pt from the platinum holder. (a) Overview of the FIB foil; white frame
237 indicates position of (b) high-angular annular dark-field (HAADF) image and EDAX spectra of
238 kerite and embedding material epoxy. (c) Detail of (b) with EDAX spectra of three inclusions,
239 interpreted as possibly chlorite and a complex Al-silicate, possibly a clay mineral. (d) Detail of
240 (b) with EDAX spectra of two inclusions, a Fe-Ca-phosphate and a complex Al-silicate.

241

242 3.6 IR spectra

243 Head et al. (2023) criticize our IR spectra and argue that we should have used modern fungal
244 chitin standards for comparison and a more detailed comparison with sub-fossil and fossil
245 fungi. Since we knew that the Volyn biota experienced temperatures near 300 °C, comparison

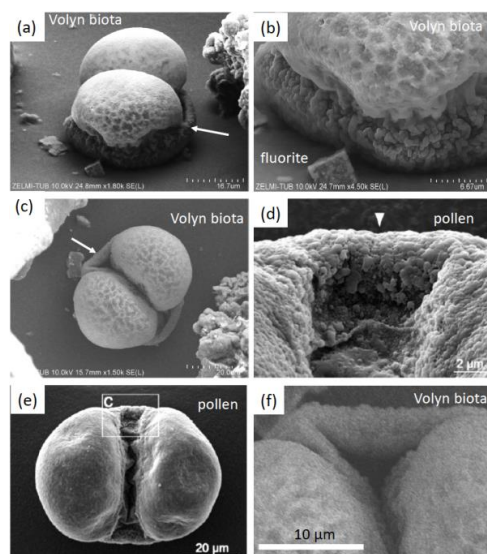


246 with modern fungi did not seem appropriate to us. Instead, we followed the procedure by
247 Loron et al. 2019) and the thermal degradation studies of chitosan (WanJun et al., 2005;
248 Zawadzki and Kaczmarek, 2010; Vasilev et al., 2019). These are clearly consistent with our
249 conclusion that chitosan is a constituent of the kerite material.

250

251 **4 Comparison of kerite morphology**

252 Head et al. (2023) present evidence for strong similarity of one object of our sample collection
253 with pollen of an extinct conifer. The similarity is indeed striking, but we want to stress
254 important differences (Fig. 6):
255



256

257 **Figure 6.** SEM images for direct comparison of kerite object from Volyn biota (a, b, c, f) and
258 *Pinus* pollen (d, e) from Head et al. (2023). Note that the kerite object is sitting firmly on base
259 consisting of OM (a, b), whereas pollen are free objects. The surface of kerite is characterized
260 by dents (b), whereas the pollen shows a microrogulate surface (d). What is described from
261 pollen as air sacs (d, e) sits on a similar height as the pollen grain itself (d), whereas what we
262 described as a sheath comes from the base of the kerite object (arrows in a and c). This sheath
263 shows some inward folding (f), which is not seen in the air sac of the pollen.

264

265 The kerite object is sitting firmly on a base consisting of OM (Fig. 6a, b), whereas pollen
266 are free objects. The surface of kerite is characterized by dents (Fig. 6b), whereas the pollen
267 shows a microrogulate surface (Fig. 6d). What is described from pollen as air sacs (Fig. 6d, e)
268 sits on a similar height as the pollen grain itself, whereas what we described as a sheath
269 from the base of the kerite object (arrows in Fig. 6a, c). This sheath shows some inward folding
270 (Fig. 6f), which is not seen in the air sac of the pollen.

271

272 The other object, which Head et al. (2023) interpret as a plant hair (figure 3 j, k, l; in Franz
273 et al. 2023a) due to the similarity to ‘museum dust’, also sits firmly on a base. If such a delicate
274 object like unfossilized trichome was transported down into the chamber (where it was
275 sampled), it is difficult to imagine that it survived the transport.

276

277 Head et al. (2023) restrict their criticism to these two objects but do not mention the fact
278 that the large majority of objects we presented has a different morphology, with filaments up
279 to the mm-size, bulbous objects, objects with irregular shape etc. None of these objects is



278 similar to trichomes. Also, they do not mention the internal structure with a channel, which
279 we documented in detail (figure 11 in Franz et al., 2023a), and which is obvious also in BSE
280 images (Fig. BSE e, f). They also do not mention the presence of Bi(Te,S) biomineralization,
281 which we documented (figure 10 in Franz et al., 2023). To the best of our knowledge, this type
282 of biomineralization was not observed in trichomes.

283

284 **5 Age of the fossils**

285 Popov (2023) questioned the minimum age of the organic matter, which we proposed as 1.5
286 Ga, based on the Ar-Ar laser ablation data (Franz et al., 2022a) of muscovite in a pseudomorph
287 after beryl. He proposed a sequence of events, starting with the intrusion of the granites and
288 the pegmatites at approximately 1.76 Ga (Shumlyanskyy et al., 2017, 2021), cooling and
289 pseudomorph formation due to a hydrothermal event at 1.5 Ga, then again cooling,
290 introduction of organic matter, then a second hydrothermal event, which converted
291 muscovite into tobelite and K-feldspar into buddingtonite. The age of the second event could
292 have been early Phanerozoic, based on our data (Franz et al., 2022b) of dating attempts of the
293 kerite itself, which produced in Popov's (2023) wording an isochrone of 493 ± 98 (1s) Ma, but
294 which we considered only as a reference line due to the large uncertainty. In this sequence of
295 events the breccia formation is missing, but this event is important: It fractionated feldspar
296 and quartz into cm-sized, irregular pieces, including a large piece of pegmatitic beryl. This
297 event must have occurred before the pseudomorph formation, because the delicate
298 pseudomorph, consisting of a rather loose framework of muscovite and bertrandite would not
299 have survived the brecciation. But the breccia is cemented by black opal (pigmented by
300 hydrocarbons), and OM must have been present before precipitation of opal. Therefore, the
301 sequence of events after the intrusion must have been: Presence of organic matter,
302 brecciation, pseudomorph formation at 1.5 Ga in one event, first with muscovite formation,
303 then during decay of the kerite and production of NH_4^+ tobelite and buddingtonite (including
304 formation of secondary, C-H bearing fluid inclusions in low-T beryl), then further cooling. It
305 was made clear in our text that "...the fluid composition changed during the pseudomorph
306 formation, starting with F-dominated K-rich fluids producing pure F-muscovite, followed by
307 alternating NH_4 -rich and K-rich compositions, producing oscillatory growth zones in
308 buddingtonite (Fig. 5e) and ending with a late K-rich fluid (producing some outer K-rich zones
309 in buddingtonite; Fig. 5d)." This is the same conclusion as in our first analysis of the
310 pseudomorph's texture (Franz et al., 2017) and clear from the summary figure 13, illustrating
311 the sequence of processes in one single geological event. We feel misinterpreted by Popov
312 (2023), who wrote that in our second study we had changed our mind.

313 There might have been additional hydrothermal events since 1.5 Ga, caused e. g. by the
314 Neoproterozoic Volyn Large Igneous Province at approximately 600 Ma or later Devonian
315 rifting of the Prypyat aulacogen (Shumlyanskyy et al., 2016), but none of these events is
316 documented up to now in the pegmatites of the Volyn field. We fully agree with Popov (2023)
317 that the late-stage development of pegmatites including later overprinting by hydrothermal
318 events may point to a protracted history. However, for the Volyn locality, the late-stage
319 development is documented in Lazarenko et al. (1973) and in a study of dissolution of Volyn
320 beryl crystals with the formation of typical and diagnostic etching (Franz et al., 2023b)

321

322 **6 Origin of kerite - biotic or abiotic**

323 Head et al. (2023) conclude their discussion with "We have doubts whether any of the in-situ
324 Volyn 'biota' is organic in origin", based on references to the low $\delta^{13}\text{C}$ values obtained via
325 experiments with Fischer-Tropsch-type synthesis under hydrothermal conditions in the



326 presence of metallic Fe. From a starting composition with an assumed value for $\delta^{13}\text{C}$ of -20 ‰,
327 different organic compounds were obtained with a rather uniform composition of -50 ‰
328 (McCollum and Seewald, 2006). Abiotic synthesis of nitrogen-bearing organic carbon species,
329 such as amino acids, is thermodynamically favored by molecular H_2 , which is produced by
330 serpentinization of Fe-rich mantle-derived rocks (Ménez et al., 2018).

331 Source for abiotic synthesis in Volyn should be the mantle with a uniform $\delta^{13}\text{C}$ value of
332 -5 ‰ (Marty et al., 2013, and references therein), because the Korosten pluton is comprised
333 mainly of mantle-derived granitic, gabbroic, and anorthositic rocks (Shumlyanskyy et al., 2017,
334 2021). Assuming a similar fractionation of -30 ‰ for a source with $\delta^{13}\text{C}$ of -5 ‰, a composition
335 of abiotic kerite should have values of -35 ‰, but many kerite bulk samples have much lower
336 values between -40‰ and -48‰. According to the model of abiotic origin, mantle-derived
337 fluids should also be the source for nitrogen. The N-isotopic signature of the mantle scatters
338 from -25 ‰ to +15, with most values around -5 ± 3 ‰ Cartigny (2005), therefore a mantle
339 source is less likely for the Volyn locale, with positive $\delta^{15}\text{N}$ values up to 10 ‰ throughout. An
340 alternative source might be the country rocks of the Korosten pluton, but this would require
341 a large amount of C- and N-rich fluids, and there is no geological evidence for such fluid-rock
342 interactions. They should have left their signature also within the granites, which are the hosts
343 of the pegmatites. The presence of Fe-rich minerals as catalyst for the production of abiotic
344 carbonaceous material in serpentinites (Nan et al., 2021) is not a good analogue for the
345 granitic environment, in which Fe-rich minerals are generally scarce. Yushkin (1996) presented
346 analyses of different proteins in kerite and used it as an argument that abiotic synthesis is
347 possible. However, he starts from the assumption of abiotic origin and did not consider the
348 possibility of fossil material. The large amounts of kerite of several kg recovered from the mine
349 (Ginzburg et al., 1987) is in our view more consistent with biomass accumulation; what has
350 been described as abiotic formation of carbonaceous material was observed in small amounts
351 in thin section only (e. g. Nan et al., 2021; Ménez et al., 2018).

352

353 **Summary and open questions**

354 Although the morphology of two objects, selected by Head et al. (2023) show a striking
355 similarity to recent organisms, the combination of all observations is much more in favor of
356 fossil organisms: The occurrence in the mine as part of the deep biosphere; a large variety of
357 morphologically different objects, which however have all the same type of rim
358 mineralization; their brittle behavior; the internal structure with a channel in the filaments;
359 the presence of biomineral inclusions of Bi(Te,S).

360 We are aware that our single age determination of 1.5 Ga for the hydrothermal
361 overprinting of the pegmatites should be verified or falsified by ages on different minerals
362 and/or different isotope systems. If more and better data will be available, we are happy to
363 change the interpretation, but with the current available data the presented interpretation
364 seems to be the best one. Fluid inclusion studies might further help to clarify the origin of
365 kerite (Vozniak et al., 2012, and references therein; Kalyuzhnyi et al., 1971). Liu et al. (2022)
366 observed whewellite ($\text{CaC}_2\text{O}_4 \cdot \text{H}_2\text{O}$) in $\text{CO}_2\text{-N}_2\text{-CH}_4$ -vapor of fluid inclusions in topaz, thought as
367 a product of oxidation of organic material with an alkaline fluid. In-situ determination of C-
368 and N-isotopes, and possibly also other stable isotopes (e. g. O, S) might also help to further
369 clarify the type of organisms, their internal structure, and their origin.

370

371



372 *Data availability.* All data are as figures in the text or in the cited references.

373

374 *Supplement.* There is no supplement to this article.

375

376 Author contributions. GF concept, figures, and writing; VK writing, FTIR; VC and PL information
377 about the sampling and occurrence, US writing, stable isotopes.

378

379 *Competing interests.* The authors declared that they have no competing interests.

380

381 *Acknowledgements.* We thank Anja Schreiber and Richard Wirth for permission to use
382 unpublished TEM data.

383

384 *Financial support.* VK acknowledges funding by Alexander von Humboldt foundation.

385

386 **References**

387

388 Barton, M. D., and Young, S. Non-pegmatitic deposits of beryllium: Mineralogy, geology, phase
389 equilibria and origin. *Reviews in Mineralogy and Geochemistry*, 50, 591-691, 2002.

390 Cartigny, P., Stable isotopes and the origin of diamond, *Elements*, 1, 79-84, 2005.

391 Ensikat, H.-J., Mustafa, A., and Weigend, M., Complex patterns of multiple biomineralization
392 in single-celled plant trichomes of the Loasaceae, *Amer. J. Botany*, 104, 195-206, 2017.

393 Franz, G., Khomenko, V., Vishnyevskyy, A., Wirth, R., Nissen, J., Rocholl A. Biologically mediated
394 crystallization of buddingtonite in the Paleoproterozoic: Organic-igneous interactions from
395 the Volyn pegmatite, Ukraine. *Amer Mineral* 102, 2119-2135, 2017.

396 Franz, G., Sudo, M., Khomenko, V. $^{40}\text{Ar}/^{39}\text{Ar}$ dating of a hydrothermal pegmatitic
397 buddingtonite-muscovite assemblage from Volyn, Ukraine. *Eur. J. Mineral.*, 34, 7-18.
398 doi.org/10.5194/ejm-34-7-2022, 2022a.

399 Franz, G., Lyckberg, P., Khomenko, V., Chournousenko, V., Schulz, H.-M., Mahlstedt, N., Wirth,
400 R., Glodny, J., Gernert, U., and Nissen, N. Fossilization of Precambrian organic matter (kerite)
401 from the Volyn pegmatite, Ukraine. *BioGeosciences*, 19, 1795-1811, 2022b.

402 Franz, G., Khomenko, V., Lyckberg, P., Chournousenko, V., Struck, U., Wirth, R., Gernert, U.,
403 Nissen, J., The Volyn biota (Ukraine) – indications for 1.5 Gyr old eucaryotes in 3D-
404 preservation, a spotlight on the ‘boring billion’. *BioGeosciences*, 20, 1901-1924,
405 doi.org/10.5194/bg-20-1901-2023, 2023a.

406 Franz, G., Vyschnevskiy, O. A., Khomenko, V. M., Lyckberg, P., and Gernert, U.: Etch pits in
407 heliodor and green beryl from the Volyn pegmatites, Northwest Ukraine: A diagnostic feature,
408 *Gems & Gemology*, 59(3) 324-339, doi.org/10.5741/GEM;S.59.3.324, 2023b.

409 Ginzburg, A.I., Bulgakov, V.S., Vasilishin, I.S., Luk'yanova, V.T., Solntseva, L.S., Urmenova, A.M.,
410 and Uspenskaya, V.A.: Kerite from pegmatites of Volyn, *Dokl. Akad. Nauk SSSR*, 292, 188–191,
411 1987 (in Russian).

412 Gorlenko, V.M., Zhmur, S.I., Duda, V.I., Osipov, G.A., Suzina, N.E., and Dmitriev, V. V.: Fine
413 structure of fossilized bacteria in Volyn kerite, *Orig. Life Evol. Biosph.*, 30, 567–577, 2000.

414 Head, M. J., Riding, J. B., O'Keefe, J. M. K., Jeiter, J., and Gravendyck, J., Comment on Franz et
415 al. 2023: A reinterpretation of the 1.5 billion year old Volyn ‘biota’ of Ukraine, and discussion
416 on the evolution of eucaryotes, *BioGeosciences*,
417 <https://egusphere.copernicus.org/preprints/2023/egusphere-2023-2748/>, 2023.



- 418 Kalyuzhnyi V. A., Voznyak, D. K., Gigashvili, G. M.: Mineral-forming fluids and mineral
419 paragenesis of chamber pegmatites of Ukraine, Kyiv: Naukova Dumka, 216 pp., 1971 (in
420 Ukrainian).
- 421 Lazarenko, E. K., Pavlishin, V. J., Latysh, V. T., and Sorokon, Ju. G.: Mineralogy and genesis of
422 the chamber pegmatites from Volyn, (in Russian) Lvov, Vysskaja shkola, 360 pp, 1973.
- 423 Liu, Y., Schmidt, C., and Li, J., Peralkalinity in peraluminous granitic pegmatites. I. Evidence
424 from whewellite and hydrogen carbonate in fluid inclusions, *Amer. Mineral*, 107, 233-238,
425 2022.
- 426 Loges, A., Manni, M., Louvel, M., Wilke, M., Jahn, S., Welter, E., Borchert, M., Qiao, S., Klemme,
427 S., and Keller, B. G., Complexation of Zr and Hf in fluoride-rich hydrothermal aqueous fluids
428 and its significance for high field strength element fractionation, *Geochim. Cosmochim. Acta*,
429 366, 167-181, doi.org/10.1016/j.gca.2023.12.013, 2023.
- 430 Loron, C. C., François, C., Rainbird, R. H., Turner, E. C., Borensztajn, S., and Javaux, E. J. Early
431 fungi from the Proterozoic era in Arctic Canada. *Nature* 570.7760: 232-235, 2019.
- 432 Lu'kyanova, V. T., Lobzova, R. V., and Popov, V. T. Filaceous kerite in pegmatites of Volyn.
433 *Izvestiya Ross. Akademii Nauk Ser. Geologicheskaya*, 5, 102-118, 1992 (in Russian).
- 434 Nan, J., King, H. E., Delen, G., Meirer, F., Weckhysen, B. M., Guo, Z., Peng, X., and Plümer, O.,
435 The nanogeochemistry of abiotic carbonaceous matter in serpentinites from the Yap Trench,
436 western Pacific Ocean, *Geology*, 49, 330-334, doi.org/10.1130/G48153.1, 2021.
- 437 Mäder, U. K., Ramseyer, K., Daniels, E. J., and Althaus, E. Gibbs free energy of buddingtonite
438 ($\text{NH}_4\text{AlSi}_3\text{O}_8$) extrapolated from experiments and comparison to natural occurrences and
439 polyedral estimation. *Eur. J. Mineral.* 8, 755-766, 1996.
- 440 Marty, B., Alexander, O'D., and Raymond, S. N., Primordial origins of Earth's carbon. *Reviews*
441 *Mineral. Geochem.*, 75, 149-181, 2013.
- 442 Ménez, B., Pisapia, C., Andreani, M., Jamme, F., Vanbellingen, Q., et al., et al. abiotic synthesis
443 of amino acids in the recesses of the oceanic lithosphere, *Nature*, 564 (7734), 59-63,
444 doi.org/10.1038/s41596-018-0684-z.hal-02111638, 2018.
- 445 McCollom, T. M., and Seewald, J. S.: Carbon isotope composition of organic compounds
446 produced by abiotic synthesis under hydrothermal conditions, *Earth Planet. Sci. Lett.* 243,
447 74-84, doi.org/10.1016/j.epsl.2006.01.027, 2006.
- 448 Mustafa, A., Ensikat, H.-J., and Weigend, M., Ontogeny and the process of biomineralization
449 in the trichomes of Laosaceae, *Amer. J. Botany*, 104(3), 367-378, 2017.
- 450 Mustafa, A., Ensikat, H.-J., and Weigend, M.: Mineralized trichomes in Boraginales: complex
451 microscale heterogeneity and simple phylogenetic patterns, *Ann. Botany*, 121, 741-751, doi:
452 10.1093/aob/mcx191, 2018.
- 453 Nan, J., King, H. E., Delen, G., Meirer, F., Weckhysen, B. M. Guo, Z., Peng, Z., and Plümper,
454 O.: The nanogeochemistry of abiotic carbonaceous matter in serpentinites from the Yap
455 Trench, western Pacific Ocean, *Geology*, 49, 330-334, doi.org/10.1130/G48153.1, 2021.
- 456 Popov, D. V.: Do pegmatites crystallise fast? A perspective from petrologically-constrained
457 isotopic dating, *Geosciences*, 13, 297, doi.org/10.3390/geosciences13100297, 2023.
- 458 Proshko, V. Ya., Bagmut, N. N., Vasilishin, I. S., and Panchenko, V. I.: Ammonium feldspars from
459 Volyn pegmatites and their radiospectroscopic properties, *Mineral. J. (Ukraine)*, 9, 67-71, 1987
460 (in Russian).
- 461 Shumlyansky, L., Nosova, A., Billström, K., Söderlund, U., Andréasson, P.-G., and
462 Kuzmenkova, O.: The U–Pb zircon and baddeleyite ages of the Neoproterozoic Volyn Large
463 Igneous Province: implication for the age of the magmatism and the nature of a crustal
464 contaminant, *Gff-Upsala*, 138(1), 17-30, 2016.



- 465 Shumlyansky L., Hawkesworth C., Billström K., Bogdanova S., Mytrokhyn O., Romer R.,
466 Dhuime B., Claesson S., Ernst R., Whitehouse M., Bilan O.: The origin of the Palaeoproterozoic
467 AMCG complexes in the Ukrainian Shield: new U-Pb ages and Hf isotopes in zircon.
468 *Precambrian Research*, 292, 216-239, 2017.
- 469 Shumlyansky, L., Franz, G., Glynn, S., Mytrokhyn, O., Voznyak, D., and Bilan O.:
470 Geochronology of granites of the western part of the Korosten AMCG complex (Ukrainian
471 Shield): implications for the emplacement history and origin of miarolitic pegmatites, *Eur. J.*
472 *Min.*, 33, 703-716, 2021.
- 473 Vasilev, A., Efimov, M., Bondarenko, G., Kozlov, V., Dzidziguri, E., and Karpacheva, G.: Thermal
474 behavior of chitosan as a carbon material precursor under IR radiation, *IOP Conf. Ser.: Mater.*
475 *Sci. Eng.*, 693, doi.org/10.1088/1757-899X/693/1/012002, 2019.
- 476 Voznyak, D.K., Khomenko, V.M., Franz, G., and Wiedenbeck, M.: Physico-chemical conditions
477 of the late stage of Volyn pegmatite evolution: Fluid inclusions in beryl studied by
478 thermobarometry and IR-spectroscopy methods, *Mineral. J. (Ukraine)*, 34, 26–38, 2012 (in
479 Ukrainian).
- 480 Wanjun T., Cunxin W., Donghua, C.: Kinetic studies on the pyrolysis of chitin and chitosan,
481 *Polym. Degrad. Stabil.*, 87, 389–394, 2005.
- 482 Yushkin, N. P. Natural polymer crystals of hydrocarbons as models of prebiological organisms,
483 *J. Crystal Growth*, no. 167, 237-247, 1996.
- 484 Zawadzki, J., and Kaczmarek, H.: Thermal treatment of chitosan in various conditions,
485 *Carbohydr. Polym.*, 80, 394-400, 2010.
- 486 Zhmur, S. I.: Origin of Cambrian fibrous kerites of the Volyn region, *Lithol. Mineral Resour.*, 38,
487 55-73, 2003.